

# Journal of Biomedical Optics

[SPIEDigitalLibrary.org/jbo](http://SPIEDigitalLibrary.org/jbo)

## **Monitoring angiogenesis using a human compatible calibration for broadband near-infrared spectroscopy**

Runze Yang  
Qiong Zhang  
Ying Wu  
Jeff F. Dunn

# Monitoring angiogenesis using a human compatible calibration for broadband near-infrared spectroscopy

Runze Yang,<sup>a,b</sup> Qiong Zhang,<sup>a,b</sup> Ying Wu,<sup>a,b</sup> and Jeff F. Dunn<sup>a,b,c</sup>

<sup>a</sup>University of Calgary, Department of Radiology, Calgary, Alberta, Canada

<sup>b</sup>University of Calgary, Hotchkiss Brain Institute, Calgary, Alberta, Canada

<sup>c</sup>University of Calgary, Experimental Imaging Centre, Calgary, Alberta, Canada

**Abstract.** Angiogenesis is a hallmark of many conditions, including cancer, stroke, vascular disease, diabetes, and high-altitude exposure. We have previously shown that one can study angiogenesis in animal models by using total hemoglobin (tHb) as a marker of cerebral blood volume (CBV), measured using broadband near-infrared spectroscopy (bNIRS). However, the method was not suitable for patients as global anoxia was used for the calibration. Here we determine if angiogenesis could be detected using a calibration method that could be applied to patients. CBV, as a marker of angiogenesis, is quantified in a rat cortex before and after hypoxia acclimation. Rats are acclimated at 370-mmHg pressure for three weeks, while rats in the control group are housed under the same conditions, but under normal pressure. CBV increased in each animal in the acclimation group. The mean CBV (%volume/volume) is  $3.49\% \pm 0.43\%$  (mean  $\pm$  SD) before acclimation for the experimental group, and  $4.76\% \pm 0.29\%$  after acclimation. The CBV for the control group is  $3.28\% \pm 0.75\%$ , and  $3.09\% \pm 0.48\%$  for the two measurements. This demonstrates that angiogenesis can be monitored noninvasively over time using a bNIRS system with a calibration method that is compatible with human use and less stressful for studies using animals. © Authors. Published by SPIE under a Creative Commons Attribution 3.0 Unported License. Distribution or reproduction of this work in whole or in part requires full attribution of the original publication, including its DOI. [DOI: [10.1117/1.JBO.18.1.016011](https://doi.org/10.1117/1.JBO.18.1.016011)]

Keywords: near-infrared spectroscopy; near infrared; hemoglobin; acclimation; cerebral blood volume; angiogenesis; hypoxia; brain.

Paper 12520TN received Aug. 13, 2012; revised manuscript received Nov. 6, 2012; accepted for publication Dec. 6, 2012; published online Jan. 11, 2013.

## 1 Introduction

Noninvasive measurements of cerebral blood volume (CBV) can be used as a marker of vascular density.<sup>1,2</sup> By quantifying vascular density, one can study the process of angiogenesis, or growing new blood vessels, which is a significant area of interest in the study of diseases such as cancer, stroke, and diabetes.<sup>3-5</sup>

Methods used to measure vessel density using CBV include magnetic resonance imaging (MRI), computed tomography (CT), positron emission tomography (PET), and single-photon emission computed tomography (SPECT).<sup>6-10</sup> Although each method has strengths, they usually require injection of contrast agents and are relatively expensive to operate. This could potentially limit the number of times the measurements can be conducted. Hence a repeatable, inexpensive method capable of quantifying changes in CBV is desirable, for both research as well as clinical practice.

We showed previously that quantitative near-infrared spectroscopy (qNIRS) via a broadband NIRS (bNIRS) system can be used to quantify tissue total hemoglobin ([tHb]) and CBV as a method of monitoring angiogenesis in rat brain.<sup>1</sup> bNIRS measures a broad near-infrared (NIR) spectrum and uses modeling of the attenuation spectra to measure tissue deoxyhemoglobin concentrations.<sup>1,11</sup> A common method of calibration for quantifying [tHb] and saturation has been called the anoxia method, which requires subjects to breathe 0% oxygen (anoxia) for approximately 50 to 60 s.<sup>1,11</sup>

This method assumes that a brief pulse of anoxia will convert all of the hemoglobin into the deoxygenated form, allowing for [tHb] to be calculated by quantifying tissue deoxyhemoglobin (HHb). CBV can then be calculated from [tHb] and large vessel hemoglobin concentration.

This type of calibration is not suitable for use in a wide range of conditions. For instance, anoxia may result in some level of hypoxic preconditioning<sup>12,13</sup> and may influence the outcome of animal studies of stroke. It is also not suitable for studies on patients since breathing 50 s of anoxic gas would not be tolerated.

We showed previously that one could substitute the anoxia pulse method with a graded hypoxia method for calibration of bNIRS.<sup>14</sup> Using the graded hypoxia calibration, [tHb] can be obtained by measuring the effects of a small, step-wise change in arterial oxygenation ( $S_aO_2$ ) on HHb concentrations. Since mild hypoxia is well tolerated, this method would broaden the applications of bNIRS. Although a previous study has validated its accuracy in measuring CBV under normal conditions,<sup>14</sup> it has yet to be proven that this method is suitable for detecting angiogenesis.

Previous studies have demonstrated that chronic hypoxia exposure produces significant angiogenesis and increases in blood vessel density.<sup>1,2,15-18</sup> We used chronic hypoxia exposure in rats as a means of stimulating angiogenesis. We show that quantifying angiogenesis in brain in a repeated, noninvasive fashion is possible with bNIRS using a graded hypoxia calibration method.

Address all correspondence: Jeff F. Dunn, University of Calgary, Department of Radiology, 3330 Hospital Drive, N.W., Calgary, AB T2N 4N1, Canada. Tel: 403-210-3886; E-mail: [dunnj@ucalgary.ca](mailto:dunnj@ucalgary.ca)

## 2 Methods

### 2.1 Broadband Near-Infrared System

The bNIRS system is custom-built using commercially available components, including an imaging spectrograph (Shamrock 303i, Andor Technology Inc., Northern Ireland), a broadband light source (Model 77501, Oriol Instruments Inc.), two multiple core silica optic fibers (Techen, USA), a charge-coupled device camera (DU420-BR-DD, Andor Technology Inc, Northern Ireland), and a data processor (Optix280, Dell, USA). After calibration using a reference neon spectrum, the NIR attenuation spectra were measured. The 740- to 810-nm region of the spectrum was assigned to HHb, and the 810- to 840-nm region was assigned to water. Absolute [HHb] was determined via the second differential method.<sup>11</sup> It was assumed that the rat brain consisted of 80% water, and that chronic hypoxia does not produce a change in water content of the rat's brain.<sup>18</sup>

Custom software that integrated the hardware components was used to perform data collection and analysis. The second differential analysis of the attenuation spectra was used to quantify HHb per volume of water.<sup>11,19</sup>

### 2.2 Graded Hypoxia Calibration

The graded hypoxia method is a modified version of previously described methods.<sup>10,20-23</sup> This calibration method assumes that if changes in arterial hemoglobin saturation ( $S_aO_2$ ) are brief, small, and gradual, there will be no accompanying changes in cerebral metabolic rate for oxygen (CMRO<sub>2</sub>), cerebral blood flow (CBF), and CBV.<sup>24</sup> Numerous studies have validated this assumption, showing that CBV, CMRO<sub>2</sub>, and CBF stayed constant during moderate hypoxemia and changed only under conditions of extreme arterial O<sub>2</sub> deficiency when  $S_aO_2$  dropped below 0.75.<sup>20,25,26</sup> The derivation of the calibration method is shown below and is detailed in a previous study.<sup>14</sup> NIRS is sensitive to largely to microvessel hemoglobin. Tissue hemoglobin oxygen saturation ( $S_tO_2$ ) measured by NIRS is composed of  $S_aO_2$ , capillary hemoglobin saturation, and venous saturation ( $S_vO_2$ ). It has been generally accepted that the contribution to blood volume is 20% arterial, 10% capillary, and 70% venous. Assuming the capillary contains equal amounts of arterial and venous blood,  $S_tO_2$  can be determined by Eq. (1):<sup>27</sup>

$$S_tO_2 = 0.25 \times S_aO_2 + 0.75 \times S_vO_2, \quad (1)$$

where  $S_tO_2$  is the tissue hemoglobin oxygen saturation,  $S_aO_2$  is the arterial oxygen saturation, and  $S_vO_2$  is the venous oxygen saturation.

The CMRO<sub>2</sub> can be calculated using the Fick principle:<sup>28</sup>

$$CMRO_2 = (S_aO_2 - S_vO_2) \times K \times CBF \times [Hb]. \quad (2)$$

The [Hb] is the total hemoglobin concentration in a large blood vessel ( $\mu M$ ), CBF is the cerebral blood flow, and  $K$  is the carrying capacity of hemoglobin.

We can express the Fick Equation via  $S_tO_2$  using Eqs. (1) and (2).  $S_tO_2$  is the oxygen saturation of hemoglobin, defined by  $[HbO]/[tHb]$ , where [HbO] is the tissue oxyhemoglobin concentration, and [tHb] is the sum of [HbO] and [HHb]. Since  $S_tO_2 = [HbO]/[tHb]$  and  $[tHb] = [HbO] + [HHb]$ ,  $S_tO_2$  can be expressed as:

$$S_tO_2 = 1 - \frac{[HHb]}{[tHb]}, \quad (3)$$

where [tHb] and [HHb] are the concentrations of tissue total hemoglobin and tissue deoxyhemoglobin measured by the bNIRS system, respectively.

Combining the three equations above, [HHb] can be expressed as follows:

$$[HHb] = [tHb] \times (1 - S_aO_2) + \left( \frac{0.75 \times CMRO_2}{K \times CBF \times [Hb]} \times [tHb] \right). \quad (4)$$

Equation (4) shows that [HHb] has a linear relationship with  $(1 - S_aO_2)$ ; since  $S_aO_2$  can be measured by a pulse oximeter, [tHb] can be determined from the slope of Eq. (4). After determining [tHb],  $S_tO_2$  can also be determined from Eq. (3). This derivation is more completely described in Zhang et al.<sup>14</sup>

Since CMRO<sub>2</sub>, CBF, and [Hb] was assumed to not change during the procedure, the "0.75CMRO<sub>2</sub>/K × CBF × [Hb]" will be constant. Tissue total hemoglobin measured using this method will not be affected by the original values for CMRO<sub>2</sub> and CBF since they do not affect the slope of this equation. An additional advantage of using this simplification is that the assumption concerning the relative compartment size of the arterial and venous system (25% arterial, 75% venous) does not influence the final value of [tHb] as the values are contained in the constant.

[tHb] can then be used to calculate cortical CBV (volume to volume) in the following way:

$$CBV(\%v/v) = \frac{[tHb] \times k1}{[Hb] \times R} \times 10^{-4}, \quad (5)$$

where [Hb] is the large vessel total hemoglobin concentration (g/L) obtained from the blood sample,  $k1$  is the molar mass of hemoglobin (64500 g/mol), and  $R$  is the ratio of small to large vessel hematocrit set at 0.61.<sup>29</sup>

## 3 Experimental Procedure

For three weeks, male Wistar rats ( $n = 7$ ) were exposed to hypobaric hypoxia maintained at  $370 \pm 2.1$  mmHg (mean  $\pm$  S.D.) using a custom built hypoxic chamber. The control rats ( $n = 4$ ) were housed under the same conditions as the hypoxia acclimated animals but not exposed to hypobaric hypoxia. CBV of all rats was determined before and after hypoxia acclimation using bNIRS. In order to minimize the influence of posthypoxic hypercapnia, which can stimulate cerebral blood flow,<sup>28</sup> postacclimated animals were measured 24 h after removal from the hypoxic chamber. It has been shown that elevated CBF will also elevate CBV.<sup>30</sup> Although we'd still be measuring an accurate CBV, a high steady state CBF would result in an overestimate of the change in CBV relative to the nonacclimated animals.

A mixture of 2% isoflurane,  $N_2$  (~68%), and  $O_2$  (~30%) was used to anaesthetize and ventilate the animals through a nose cone. A heated water bed and rectal thermometer was used to maintain body temperature at 37°C to 38°C. A pulse oximeter was used to measure heart rate and  $S_aO_2$  (Model 8600; Nonin, Inc., USA).

A blood gas analyzer (Stat Profile CCX, Nova Biomedical Corporation, USA) was used to analyze blood (200  $\mu\text{L}$ ) obtained from the tail vein. Depilatory cream (Nair Church & Dwight Co., Inc. USA) was used to remove fur on the head. Along the midline and approximately 5-mm anterior of the interaural line, the bNIRS optode was pressed onto the scalp, with 7-mm lateral distance between the source and detector. The cortical area, retrosplenial dysgranular cortex and lateral parietal association cortex were the primary components of the detected area.

Following the baseline measurement, the inspired oxygen fraction ( $\text{FiO}_2$ ) was decreased by decreasing  $\text{O}_2/\text{N}_2$  gas ratio so that hypoxia is induced.  $S_a\text{O}_2$  was initially reduced by 5% and sustained briefly; within 5 to 10 min,  $S_a\text{O}_2$  and  $\text{FiO}_2$  were slowly restored to baseline. The reduction and step-wise increase of the  $\text{FiO}_2$  was controlled by a computer (SAR 830/P Ventilator, IITC Life Science Inc., USA). The pulse oximeter was time-synced with the bNIRS system by a data acquisition and analysis workstation (MP150 system, BIOPAC Inc. USA).

All experiments has been approved by the Animal Care Committee at the University of Calgary and conformed to guidelines established by the Canadian Council on Animal Care. A paired *t*-test was used to compare CBV before and after acclimation for both the experimental and the control groups, where  $p < 0.05$  was considered significant.

#### 4 Results

Broadband attenuation spectra were obtained from the head of the anesthetized rat at the same time as data were obtained on arterial hemoglobin saturation using a pulse oximeter. The arterial hemoglobin saturation was reduced to 5% to 6% below baseline values, and then restored gradually. The graded hypoxia calibration took approximately 11 min. Figure 1 shows a representative time course of [HHb] and the calculated  $1 - S_a\text{O}_2$  as the inspired oxygen fraction ( $\text{FiO}_2$ ) was increased to normoxia in a step-wise fashion. In Fig. 1, the initial  $S_a\text{O}_2$  declined by 6%. Based on Eq. (4) a plot of [HHb] versus  $(1 - S_a\text{O}_2)$  will result in a slope that equals [tHb]. A sample dataset is shown in Fig 2. These data were from the same animals used in Fig. 1.

The calculation of CBV [Eq. (5)] requires [tHb], [Hb], and an estimate of large to small vessel hematocrit. Table 1 shows the physiological variables used in addition to the NIRS measure of [tHb], for the calculation of CBV; these parameters were measured by analyzing the blood from a tail vein using a blood gas analyzer. There were significant differences between the control and acclimation groups in large vessel hemoglobin content and hematocrit.

Table 1 shows the increase in CBV in the cortex for all animals due to a three-week chronic hypoxia exposure ( $n = 7$ ). Changes in CBV for control and hypoxia-acclimated rats are illustrated in Fig. 3. The mean CBV in the hypoxia acclimated group was increased by 36% ( $p < 0.001$ ). There were no significant differences in CBV values between the two time points in the control group ( $n = 4$ ,  $p > 0.05$ ). There was a 12% increase in  $S_r\text{O}_2$  ( $p < 0.05$ ) in the hypoxia acclimated group. There were no significant differences in  $S_r\text{O}_2$  in the control group.

#### 5 Discussion

The graded hypoxia calibration has a great advantage compared to the anoxia pulse technique used to quantify bNIRS signal. A small, 5% to 6% decline in  $S_a\text{O}_2$  provides a reasonable dynamic

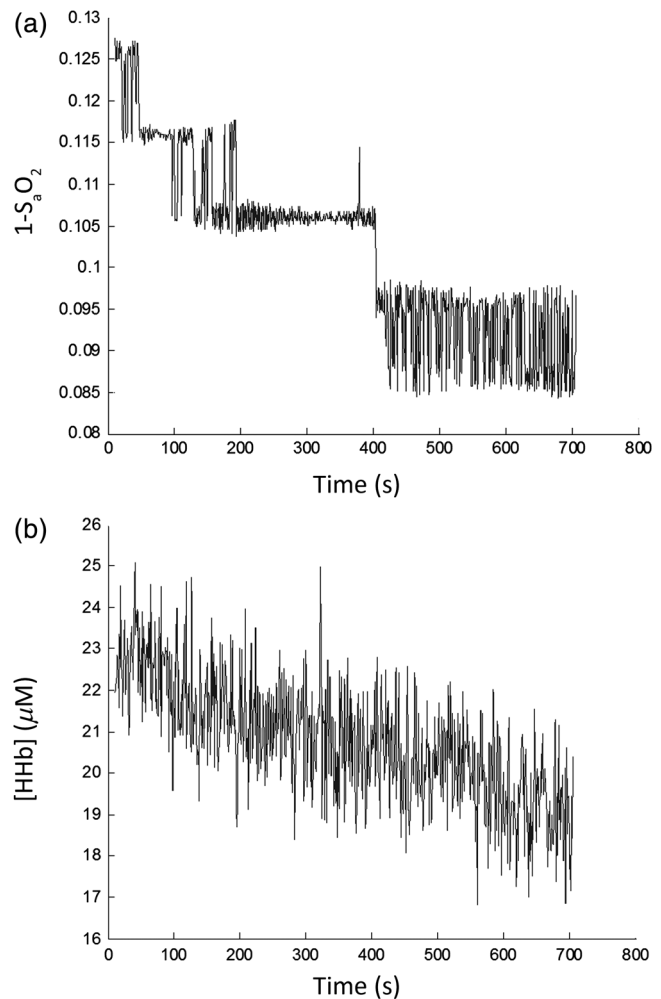


**Fig. 1** An example of arterial saturation ( $S_a\text{O}_2$ ) and NIRS based HHb concentration during graded hypoxia. Graded hypoxia was induced by reducing inspired  $\text{O}_2$ , using a computer controlled gas mixer (see methods). (a) The step-wise decrease of  $1 - S_a\text{O}_2$  is shown. In this case,  $S_a\text{O}_2$  was reduced to 0.875, and gradually increased back up to baseline. (b) Time synced corresponding decrease in [HHb] that occurred as the  $\text{FiO}_2$  was incrementally decreased.

range, which is well tolerated by humans.<sup>24</sup> This method is less stressful compared with the anoxia method where the subjects have to breathe 0% oxygen for an extended period.<sup>1,15,24</sup>

The graded hypoxia method of calibration was slightly more difficult to implement compared with the anoxia pulse method. The graded hypoxia method requires approximately 10 min more time than anoxia pulse method; it requires a sensitive pulse oximeter and a way of controlling inspired gas. For repeated studies using many subjects, one could even use pre-mixed gases, replacing the need for a gas mixer. In addition, the [Hb] needs to be known. For the general population, this value could be assumed to be 15 g/dL. In the current study, hypoxia is known to stimulate production of erythrocytes and increase hematocrit and [Hb]. In such studies, where [Hb] may change, a large vessel (venous or arterial) blood sample is needed to quantify [Hb] to control for any variation in hematocrit or [Hb].

The model is based on Eq. (4), which has grouped five variables into one constant that is assumed not to change during the calibration. In order to gain some confidence that the model is valid, we substituted for the variables using data on rat brain for

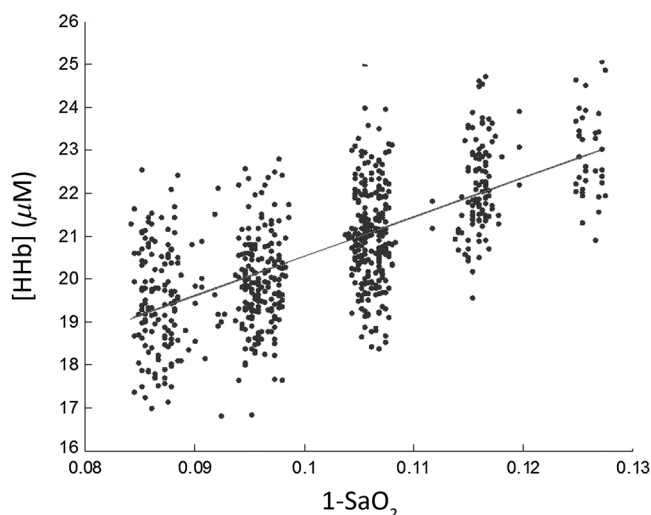


**Fig. 2** A representative linear regression between [HHb] and  $1-S_aO_2$  during the graded hypoxia process in one animal. The regression of the line is  $y = 91.38x + 11.4$ . The clustered data for  $S_aO_2$  is a result of the step-wise decline in inspired  $O_2$ . The slope of the line represents the total hemoglobin concentration ( $\mu M$ ).

CBF,  $CMRO_2$  (Ref. 31) as well as [Hb], hemoglobin carrying capacity (1.34 mL  $O_2$ /g Hb),<sup>32</sup> and [Hb]. With this substitution, the calculated intercept is 13.6 versus the observed average value of  $12.2 \pm 3.96$  (mean  $\pm$  SD). The calculated value falls within one standard deviation of the values in observed in our study. The slight deviation from the expected value is likely to be accounted for by the fact that literature values were used. The model can be derived as on physiological principles,<sup>24</sup> but this calculation provides additional evidence of its validity. For the purposes of actually calculating the CBV, these parameters do not need to be measured because they do not influence the slope.

A preacclimation CBV value of  $3.41\% \pm 0.54\%$  was determined, which is in good agreement with the 3.8% measured using radioactively labeled red blood cells and plasma, 3.26% measured with the anoxia calibration method using a bNIRS system, and 3% measured with MRI using contrast agents.<sup>1,2,33</sup>

We were able to detect increases in vascular density in all animals exposed to chronic hypoxia but saw no significant changes in the control group (Fig. 1). The 36% percent increase is in good agreement with a 31% increase in a previous study with bNIRS, which used anoxia to quantify hypoxia induced changes in CBV,<sup>1</sup> a 29% and 30% increase in capillary density,

both measured using histology.<sup>1,15,17</sup> This is lower than the 57% increase previously reported,<sup>2</sup> which may be explained by the altitude difference at which the experiments have been carried out. The good agreement with previous literature values suggests that the graded hypoxia method is sensitive enough to monitor changes in CBV.

After hypoxia acclimation, the hemoglobin saturation in the microvasculature ( $S_tO_2$ ) increased (Table 1). The effect of acclimation on tissue oxygenation has been modeled and predicts an increase in hemoglobin saturation.<sup>34</sup> Direct measurements of tissue  $PO_2$  undertaken at sea level reported a 238% increase in tissue  $PO_2$  (Ref. 16). A study using the same technique carried out in the Calgary reported a  $PO_2$  increase of 35%.<sup>35</sup> Using the rat oxy-hemoglobin dissociation curve, the predicted change in  $PO_2$  with a change in hemoglobin saturation from 72% to 82% would be 51 to 64 mmHg (25%).<sup>36</sup> This is lower than the observed changes in  $PO_2$ , but that is expected given the fact that increased capillary density will also contribute to the increased tissue  $PO_2$  (Ref. 34).

This calibration method can be applied to many types of diseased animal models, including stroke. This calibration can also be used with a wide variety of drugs, as long as  $CMRO_2$  and CBF are maintained at a steady state during the calibration procedure. The absolute values of  $CMRO_2$  and CBF before and after the calibration method will not affect the calculation of tissue total hemoglobin, as they are contained in the constant and do not have an impact on the slope. However, under conditions where the  $CMRO_2$  or CBF is subject to change in the middle of the calibration, such as during an episode of seizure, this method will not work since the slope of the regression will be affected.

There is a limitation with estimating CBV using any noninvasive NIRS method. The fact that NIRS signals originate from both brain and the skull, which can induce error, as the CBV obtained is the average blood volume in the brain and skull. In conditions where angiogenesis will only occur in the brain but not in the skull, this method can underestimate the calculated CBV. However, this will only reduce the sensitivity of this method in detecting CBV changes.

There are other quantitative NIRS methods, such as the frequency domain (FD)<sup>37,38</sup> and the time resolved (TRS) NIRS,<sup>39,40</sup> which can provide quantitative hemoglobin data. The FD method operates on the theory that changes in source detector distance will result in changes in the time average ( $R_{ac}$ ), modulation amplitude ( $R_{dc}$ ), and phase shift ( $R_{\phi}$ ) of a sinusoidal wave. By varying the source detector distances and plotting them against each of these three parameters,  $\mu_a$  and  $\mu_s$  can be solved using the slopes of these three regressions.<sup>41</sup> The TRS method utilizes the relationship between the amount of

**Table 1** Physiological parameters and calculated CBV (mean  $\pm$  SD).

	Condition	Weight (g)	Hematocrit (%)	[Hb] (g/L)	$S_tO_2$ (%)	CBV (%)
Control $n = 4$	Pre	$356 \pm 37$	$49.5 \pm 5.7$	$165.0 \pm 19.7$	$72.4 \pm 5.1$	$3.28 \pm 0.75$
	Post	$447 \pm 29$	$48.0 \pm 3.9$	$164.8 \pm 17.9$	$70.8 \pm 1.0$	$3.09 \pm 0.48$
Hypoxia Acclimation $n = 7$	Pre	$327 \pm 23$	$46.9 \pm 4.6$	$156.5 \pm 15.2$	$73.5 \pm 3.8$	$3.49 \pm 0.43$
	Post	$381 \pm 9$	$61.0 \pm 4.4^a$	$202.4 \pm 14.4^a$	$82.4 \pm 5.3^a$	$4.76 \pm 0.29^b$

<sup>a</sup>Significantly different from the preacclimation values,  $p < 0.05$ .

<sup>b</sup>Significantly different from the preacclimation values,  $p < 0.001$ .

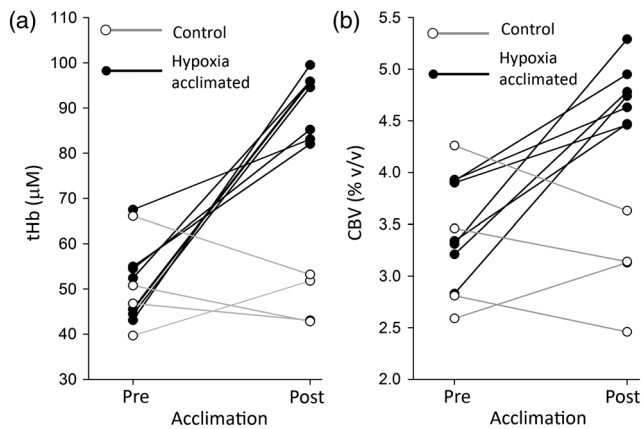


**Fig. 3** Changes in [tHb] and CBV in individual rat cortex. Changes in CBV are expected to reflect changes in microvascular density (or volume). Each animal was measured before and after hypoxia acclimation, and each line represents one animal (control, open circles, hypoxia acclimated, closed circles). Control animals were housed in similar conditions as the hypoxia group, but were not exposed to hypobaric hypoxia. (a) The total hemoglobin (tHb) in control animals did not change; in the hypoxia acclimated group, each animal showed an increase in tHb. (b) The CBV in control animals did not change; in hypoxia acclimated animals, each animal showed an increase in CBV.

time it takes for photons to reach the detector (time of flight) and depth of the tissue penetrated.<sup>42</sup> By analyzing the distribution of the time of flight for the diffusely reflected light, one is able to calculate pathlength,  $\mu_a$  and  $\mu_s$ .<sup>43</sup> The two qNIRS systems mentioned above have been validated in numerous studies.<sup>44-47</sup> The graded hypoxia calibration provides a third method of quantification for use in broadband systems.

Quantification of total hemoglobin as a marker of blood volume in human subjects using a NIRS system has significant advantages. Compared with MRI, CT, and PET, the low cost and noninvasive nature of NIRS allows it to be used in a wide population. Furthermore, since NIRS is portable, measurements can be made at bedside, which greatly benefits patients who cannot be mobilized. Broadband NIRS has some advantages compared with other qNIRS systems. Since a broadband system utilizes the entire absorption spectrum, it leads to the possibility of using the system for simultaneous detection of other absorbing or fluorescing compounds. This would include cytochrome oxidase,<sup>48</sup> an important indicator of metabolism, fibrin formation,<sup>49</sup> which play a key role in thrombosis, and even activated endothelia binding peptides labeled with NIRS fluorescent probes to monitor inflammation.<sup>13</sup>

This study illustrates that changes in CBV as a result of angiogenesis can be accurately quantified over a time-course in individual subjects using a bNIRS system in a manner that can be translated to humans and is less stressful for animal studies.

### Acknowledgments

This work was partially supported by an NIH RO1 EB002085, by the Canadian Institutes of Health Research FIN 79260, the Canadian Foundation for Innovation and the Alberta Innovates Health Solutions

### References

1. J. F. Dunn et al., "Monitoring angiogenesis noninvasively with near-infrared spectroscopy," *J. Biomed. Opt.* **13**(6), 064043 (2008).

2. J. F. Dunn et al., "Monitoring angiogenesis in brain using steady-state quantification of DeltaR2 with MION infusion," *Magn. Reson. Med.* **51**(1), 55–61 (2004).
3. G. K. Kolluru, S. C. Bir, and C. G. Kevil, "Endothelial dysfunction and diabetes: effects on angiogenesis, vascular remodeling, and wound healing," *Int. J. Vasc. Med.* **2012** (2012).
4. P. M. Hoff and K. K. Machado, "Role of angiogenesis in the pathogenesis of cancer," *Cancer Treat. Rev.* **38**(7), 825–833 (2012).
5. A. Ergul, A. Alhusban, and S. C. Fagan, "Angiogenesis: A harmonized target for recovery after stroke," *Stroke* **43**(8), 2270–2274 (2012).
6. T. S. Leung et al., "A new method for the measurement of cerebral blood volume and total circulating blood volume using near infrared spatially resolved spectroscopy and indocyanine green: application and validation in neonates," *Pediatr. Res.* **55** (1), 134–141 (2004).
7. D. W. Brown et al., "Quantitative near infrared spectroscopy measurement of cerebral hemodynamics in newborn piglets," *Pediatr. Res.* **51**(5), 564–570 (2002).
8. E. Henderson et al., "Simultaneous MRI measurement of blood flow, blood volume, and capillary permeability in mammary tumors using two different contrast agents," *J. Magn. Reson. Imag.* **12**(6), 991–1003 (2000).
9. P. Hopton, T. S. Walsh, and A. Lee, "Measurement of cerebral blood volume using near-infrared spectroscopy and indocyanine green elimination," *J. Appl. Physiol.* **87**(5), 1981–1987 (1999).
10. J. P. Muizelaar, P. P. Fatouros, and M. L. Schroder, "A new method for quantitative regional cerebral blood volume measurements using computed tomography," *Stroke* **28**(10), 1998–2005 (1997).
11. S. J. Matcher and C. E. Cooper, "Absolute quantification of deoxyhemoglobin concentration in tissue near infrared spectroscopy," *Phys. Med. Biol.* **39**(8), 1295–1312 (1994).
12. B. K. Wacker, T. S. Park, and J. M. Gidday, "Hypoxic preconditioning-induced cerebral ischemic tolerance: role of microvascular sphingosine kinase 2," *Stroke* **40**(10), 3342–3348 (2009).
13. K. Park et al., "A new atherosclerotic lesion probe based on hydrophobically modified chitosan nanoparticles functionalized by the atherosclerotic plaque targeted peptides," *J. Control. Release* **128**(3), 217–223 (2008).
14. Q. Zhang et al., "A near-infrared calibration method suitable for quantification of broadband data in humans," *J. Neurosci. Methods* **188**(2), 181–186 (2010).
15. J. A. Boero et al., "Increased brain capillaries in chronic hypoxia," *J. Appl. Physiol.* **86**(4), 1211–1219 (1999).
16. J. F. Dunn et al., "Noninvasive assessment of cerebral oxygenation during acclimation to hypobaric hypoxia," *J. Cereb. Blood Flow Metab.* **20**(12), 1632–1635 (2000).
17. J. F. Dunn et al., "Training the brain to survive stroke," *PLoS One* **7**(9), e45108 (2012).
18. J. C. LaManna, L. M. Vendel, and R. M. Farrell, "Brain adaptation to chronic hypobaric hypoxia in rats," *J. Appl. Physiol.* **72**(6), 2238–2243 (1992).
19. R. Springett et al., "Oxygen dependency and precision of cytochrome oxidase signal from full spectral NIRS of the piglet brain," *Am. J. Physiol. Heart Circ. Physiol.* **279**(5), H2202–H2209 (2000).
20. J. S. Wyatt et al., "Quantitation of cerebral blood volume in human infants by near-infrared spectroscopy," *J. Appl. Physiol.* **68**(3), 1086–1091 (1990).
21. T. Wolf et al., "Noninvasive near infrared spectroscopy monitoring of regional cerebral blood oxygenation changes during peri-infarct depolarizations in focal cerebral ischemia in the rat," *J. Cereb. Blood Flow Metab.* **17**(9), 950–954 (1997).
22. M. J. Van de Ven et al., "Can cerebral blood volume be measured reproducibly with an improved near infrared spectroscopy system?," *J. Cereb. Blood Flow Metab.* **21**(2), 110–113 (2001).
23. N. C. Brun et al., "Near-infrared monitoring of cerebral tissue oxygen saturation and blood volume in newborn piglets," *Am. J. Physiol.* **273**(2 Pt. 2), H682–686 (1997).
24. C. E. Elwell et al., "Quantification of adult cerebral hemodynamics by near-infrared spectroscopy," *J. Appl. Physiol.* **77**(6), 2753–2760 (1994).
25. K. Kogure et al., "Mechanisms of cerebral vasodilatation in hypoxia," *J. Appl. Physiol.* **29**(2), 223–229 (1970).

26. H. Johansson and B. K. Siesjo, "Cerebral blood flow and oxygen consumption in the rat in hypoxic hypoxia," *Acta Physiol Scand* **93**(2), 269–276 (1975).
27. K. M. Tichauer et al., "Measurement of cerebral oxidative metabolism with near-infrared spectroscopy: a validation study," *J. Cereb. Blood Flow Metab.* **26**(5), 722–730 (2005).
28. D. W. Brown, J. Hadway, and T. Y. Lee, "Near-infrared spectroscopy measurement of oxygen extraction fraction and cerebral metabolic rate of oxygen in newborn piglets," *Pediatr. Res.* **54**(6), 861–867 (2003).
29. D. Bereczki et al., "Hypoxia increases velocity of blood flow through parenchymal microvascular systems in rat brain," *J. Cereb. Blood Flow Metab.* **13**(3), 475–486 (1993).
30. T. S. Leung et al., "Estimating a modified Grubb's exponent in healthy human brains with near infrared spectroscopy and transcranial Doppler," *Physiol. Meas.* **30**(1), 1–12 (2009).
31. M. Hagerdal et al., "The effect of induced hypothermia upon oxygen consumption in the rat brain," *J. Neurochem.* **24**(2), 311–316 (1975).
32. F. Xu, Y. Ge, and H. Lu, "Noninvasive quantification of whole-brain cerebral metabolic rate of oxygen (CMRO<sub>2</sub>) by MRI," *Magn. Reson. Med.* **62**(1), 141–148 (2009).
33. W. Lin et al., "Quantitative magnetic resonance imaging in experimental hypercapnia: improvement in the relation between changes in brain R<sub>2</sub> and the oxygen saturation of venous blood after correction for changes in cerebral blood volume," *J. Cereb. Blood Flow Metab.* **19**(8), 853–862 (1999).
34. O. Y. Grinberg et al., "Modeling of the response of pO<sub>2</sub> in rat brain to changes in physiological parameters," *Adv. Exp. Med. Biol.* **566**, 111–118 (2005).
35. E. Ortiz-Prado et al., "A method for measuring brain partial pressure of oxygen in unanesthetized unrestrained subjects: the effect of acute and chronic hypoxia on brain tissue PO<sub>2</sub>," *J. Neurosci. Methods* **193**(2), 217–225 (2010).
36. C. F. Cartheuser, "Standard and pH-affected hemoglobin-O<sub>2</sub> binding curves of Sprague-Dawley rats under normal and shifted P50 conditions," *Comp. Biochem. Physiol. Comp. Physiol.* **106**(4), 775–782 (1993).
37. D. M. Hueber et al., "Noninvasive and quantitative near-infrared haemoglobin spectrometry in the piglet brain during hypoxic stress, using a frequency-domain multidistance instrument," *Phys. Med. Biol.* **46**(1), 41–62 (2001).
38. M. A. Franceschini et al., "Assessment of infant brain development with frequency-domain near-infrared spectroscopy," *Pediatr. Res.* **61**(5 Pt. 1) 546–551 (2007).
39. N. Yokose et al., "Bedside monitoring of cerebral blood oxygenation and hemodynamics after aneurysmal subarachnoid hemorrhage by quantitative time-resolved near-infrared spectroscopy," *World Neurosurg.* **73**(5), 508–513 (2010).
40. N. Yokose et al., "Bedside assessment of cerebral vasospasms after subarachnoid hemorrhage by near infrared time-resolved spectroscopy," *Adv. Exp. Med. Biol.* **662**, 505–511 (2010).
41. S. Fantini et al., "Noninvasive optical monitoring of the newborn piglet brain using continuous-wave and frequency-domain spectroscopy," *Phys. Med. Biol.* **44**(6), 1543–1563 (1999).
42. H. Wabnitz et al., "Time-resolved near-infrared spectroscopy and imaging of the adult human brain," *Adv. Exp. Med. Biol.* **662**, 143–148 (2010).
43. M. S. Patterson, B. Chance, and B. C. Wilson, "Time resolved reflectance and transmittance for the noninvasive measurement of tissue optical properties," *Appl. Opt.* **28**(12), 2331–2336 (1989).
44. R. Gatto et al., "Frequency domain near-infrared spectroscopy technique in the assessment of brain oxygenation: a validation study in live subjects and cadavers," *J. Neurosci. Methods* **157**(2), 274–277 (2006).
45. K. Sakatani et al., "[Progress in NIRS monitoring of cerebral blood flow]," *Brain Nerve* **63**(9), 955–961 (2011).
46. N. Roche-Labarbe et al., "Noninvasive optical measures of CBV, StO<sub>2</sub>, CBF index, and rCMRO<sub>2</sub> in human premature neonates' brains in the first six weeks of life," *Hum Brain Mapp.* **31**(3), 341–352 (2010).
47. R. Re et al., "A compact time-resolved system for near infrared spectroscopy based on wavelength space multiplexing," *Rev. Sci. Instrum.* **81**(11), 113101 (2010).
48. C. E. Cooper et al., "Steady state redox levels in cytochrome oxidase: relevance for in vivo near infrared spectroscopy (NIRS)," *Adv. Exp. Med. Biol.* **645**, 123–128 (2009).
49. Y. Zhang et al., "In vivo near-infrared imaging of fibrin deposition in thromboembolic stroke in mice," *PLoS One* **7**(1), e30262 (2012).